# Metal-semiconductor transition in the supercooled liquid phase of the $Ge_2Sb_2Te_5$ and GeTe compounds
# Supplemental Material

M. Cobelli, D. Dragoni,* S. Caravati, and M. Bernasconi

*Dipartimento di Scienza dei Materiali, Università di Milano-Bicocca,*

*Via R. Cozzi 55, I-20125, Milano, Italy*

| $T$ | $A_v$ | $E_v$ | $A_c$ | $E_c$ |
|---|---|---|---|---|
| $K$ | $\times 10^{-3} eV^{-1}$Å$^{-3}$ | $eV$ | $\times 10^{-3} eV^{-1}$Å$^{-3}$ | $eV$ |
| 898 | 19.43 | 0.07 | 13.97 | -0.02 |
| 848 | 19.33 | 0.01 | 14.12 | 0.03 |
| 796 | 19.72 | 0.04 | 15.34 | 0.16 |
| 696 | 20.42 | 0.04 | 15.42 | 0.26 |
| 591 | 20.69 | -0.05 | 15.85 | 0.32 |
| 499 | 21.40 | -0.06 | 15.73 | 0.34 |

Table. SI. Fitting parameters of the electronic density of states for GST at different temperatures with the rVV10 functional. The conduction and valence band edges are fitted with the square-root functions $A_c\sqrt{E-E_c}$ and $A_v\sqrt{E_v-E}$.

| $T$ | $A_v$ | $E_v$ | $A_c$ | $E_c$ |
|---|---|---|---|---|
| $K$ | $\times 10^{-3} eV^{-1}$Å$^{-3}$ | $eV$ | $\times 10^{-3} eV^{-1}$Å$^{-3}$ | $eV$ |
| 897 | 18.85 | 0.16 | 11.90 | -0.18 |
| 801 | 19.86 | 0.06 | 13.30 | 0.04 |
| 751 | 19.25 | 0.09 | 13.79 | 0.12 |
| 703 | 20.55 | -0.01 | 14.56 | 0.18 |
| 601 | 20.80 | -0.02 | 14.49 | 0.24 |
| 503 | 21.37 | -0.06 | 14.50 | 0.27 |

Table. SII. Fitting parameters of the electronic density of states for GeTe at different temperatures with the rVV10 functional. The conduction and valence band edges are fitted with the square-root functions $A_c\sqrt{E-E_c}$ and $A_v\sqrt{E_v-E}$.

| $T$ | $A_v$ | $E_v$ | $A_c$ | $E_c$ |
|---|---|---|---|---|
| $K$ | $\times 10^{-3} eV^{-1}$Å$^{-3}$ | $eV$ | $\times 10^{-3} eV^{-1}$Å$^{-3}$ | $eV$ |
| 816 | 16.98 | 0.20 | 12.08 | -0.26 |
| 741 | 17.94 | 0.15 | 13.64 | 0.05 |
| 663 | 18.56 | 0.05 | 14.58 | 0.16 |
| 583 | 19.52 | 0.01 | 14.75 | 0.27 |
| 504 | 19.17 | -0.03 | 15.79 | 0.35 |
| 382 | 19.94 | -0.08 | 16.96 | 0.46 |

Table. SIII. Fitting parameters of the electronic density of states for GST at different temperatures with the PBE functional. The conduction and valence band edges are fitted with the square-root functions $A_c\sqrt{E-E_c}$ and $A_v\sqrt{E_v-E}$.

| $T$ | $A_v$ | $E_v$ | $A_c$ | $E_c$ |
|---|---|---|---|---|
| $K$ | $\times 10^{-3} eV^{-1}$Å$^{-3}$ | $eV$ | $\times 10^{-3} eV^{-1}$Å$^{-3}$ | $eV$ |
| 950 | 15.85 | 0.36 | 10.25 | -0.78 |
| 902 | 17.50 | 0.23 | 11.13 | -0.50 |
| 804 | 17.95 | 0.17 | 11.57 | -0.17 |
| 699 | 18.37 | 0.10 | 13.14 | 0.13 |
| 602 | 19.74 | 0.02 | 13.77 | 0.29 |
| 501 | 19.59 | -0.04 | 14.93 | 0.32 |

Table. SIV. Fitting parameters of the electronic density of states for GeTe at different temperatures with the PBE functional. The conduction and valence band edges are fitted with the square-root functions $A_c\sqrt{E-E_c}$ and $A_v\sqrt{E_v-E}$.

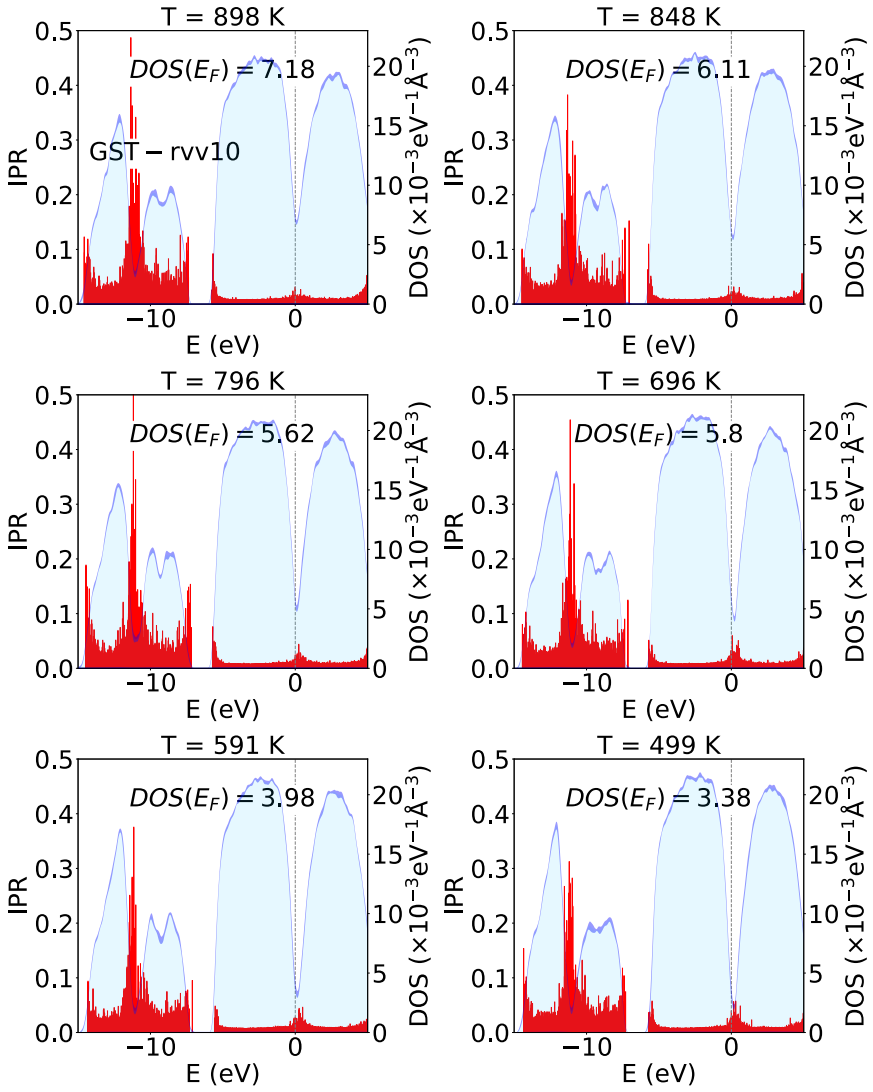


Fig. S1. Electronic density of states (DOS) of the liquid and supercooled liquid $Ge_2Sb_2Te_5$ models generated with the rVV10 functional at different temperatures. The DOS are obtained from Kohn-Sham (KS) energies computed with the HSE06 functional and broadened with Gaussian functions 27 meV wide. The DOS is averaged over nine configurations at each temperature, the DOS of the different configurations are aligned at the highest occupied state. Standard deviations are depicted by the blue shaded area around the solid lines. Different alignments of the DOS were also checked (see Section II in the article). The zero of energy is the Fermi level assigned by the average DOS at each temperature and the constraint on the total number of electrons. The Inverse participation Ratio (IPR) is superimposed. The IPR refer to the same nine configurations used to compute the DOS. The value of the DOS at the Fermi level is given in each panel. The DOS in the range -5/0 eV is due to p states of Te, Ge and Sb atoms. The DOS in the range -15/-7 eV is due to Ge, Sb 4s states and to Te 5s states.

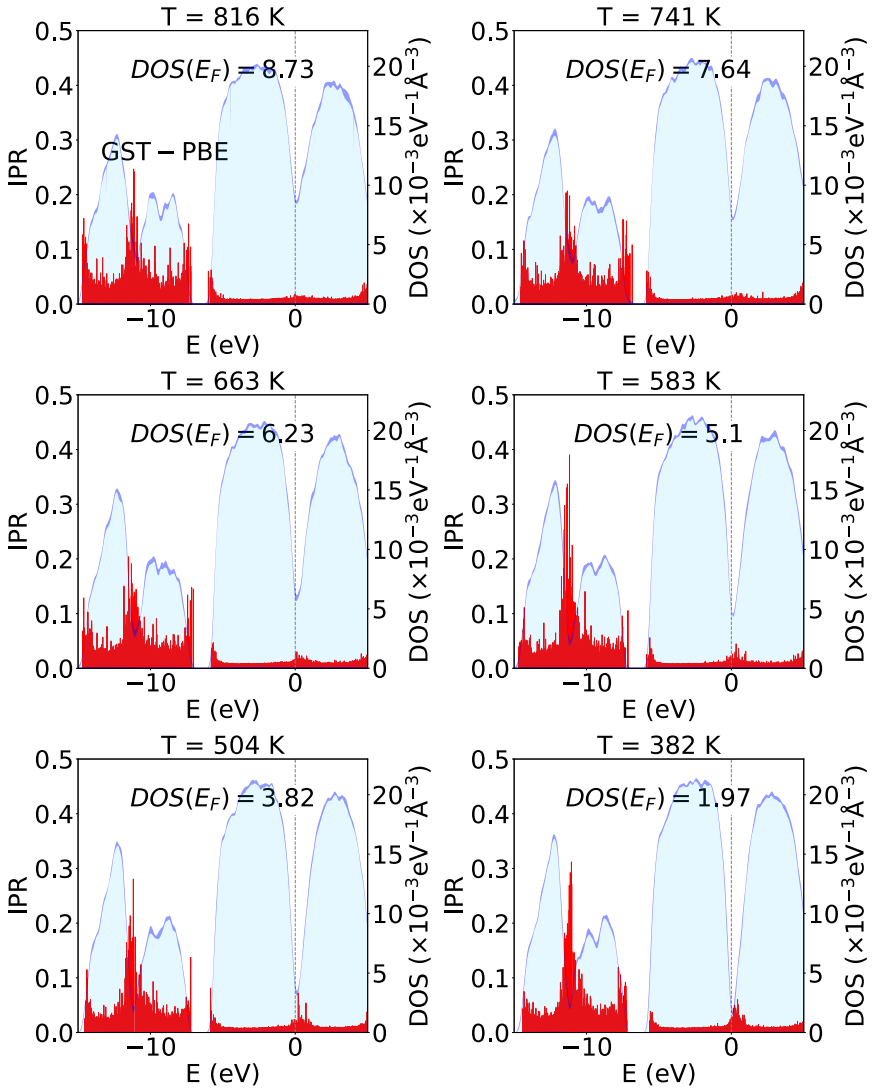


Fig. S2. Electronic density of states (DOS) of the liquid and supercooled liquid $Ge_2Sb_2Te_5$ models generated with the PBE functional at different temperatures. The DOS are obtained from Kohn-Sham energies computed with the HSE06 functional and broadened with Gaussian functions 27 meV wide. The DOS is averaged over nine configurations at each temperature, the DOS of the different configurations are aligned at the highest occupied state. Standard deviations are depicted by the blue shaded area around the solid lines. Different alignments of the DOS were also checked (see Section II in the article). The zero of energy is the Fermi level assigned by the average DOS at each temperature and the constraint on the total number of electrons. The Inverse participation Ratio (IPR) is superimposed. The IPR refers to the same nine configurations used to compute the DOS. The value of the DOS at the Fermi level is given in each panel.

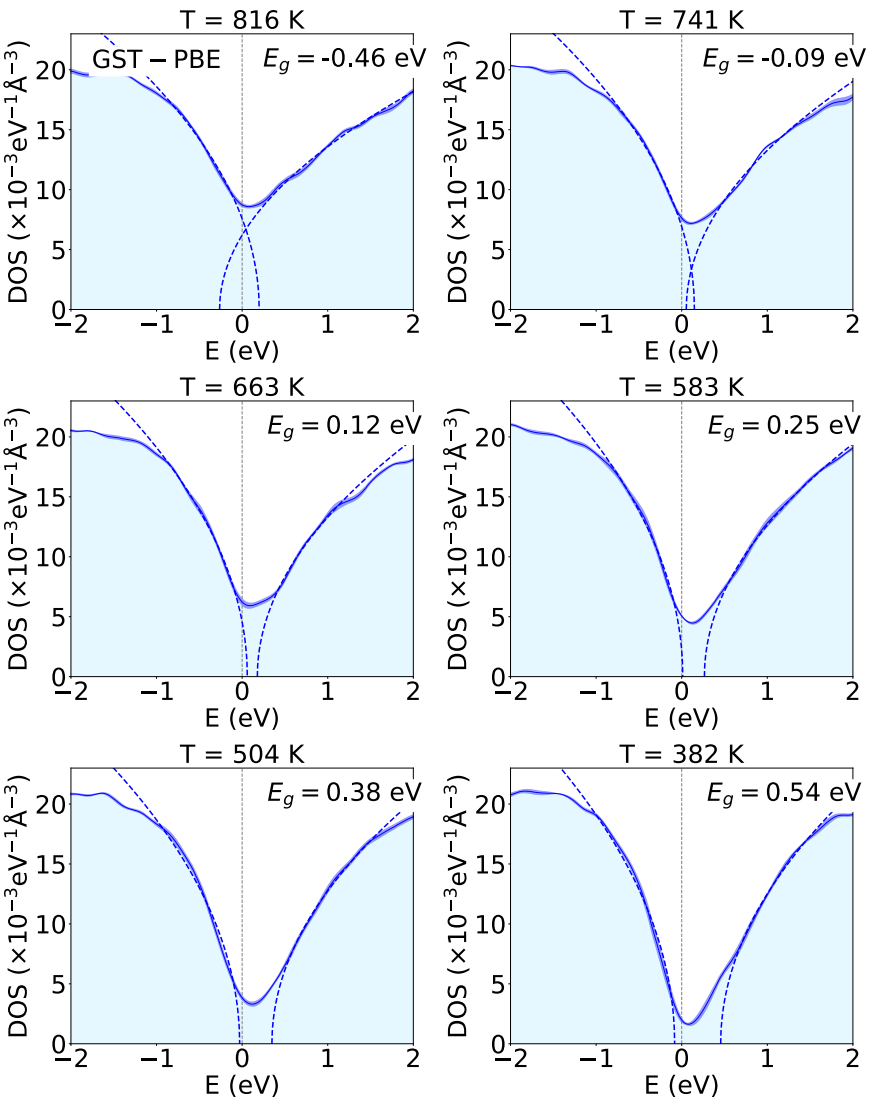


Fig. S3. Electronic density of states (DOS) around the Fermi level of the liquid and supercooled $Ge_2Sb_2Te_5$ liquid models generated with the PBE functional at different temperatures (see Fig. S2). The DOS is averaged over nine configurations at each temperature, the DOS of the different configurations are aligned at the highest occupied state. Standard deviations are depicted by the blue shaded area around the solid lines. Different alignments of the DOS were also checked (see Section II in the article). The zero of energy is the Fermi level assigned by the average DOS at each temperature and the constraint on the total number of electrons. The fitting of the valence and conduction band edges with the square-root function $A_c\sqrt{E - E_c}$ and $A_v\sqrt{E_v - E}$ in the gray shaded regions are also shown (dashed lines). The fitting parameters $A_v$, $E_v$, $A_c$ and $E_c$ are given in Table SIII above. The resulting band gap $E_g$=$E_c$ -$E_v$ is given in each panel.

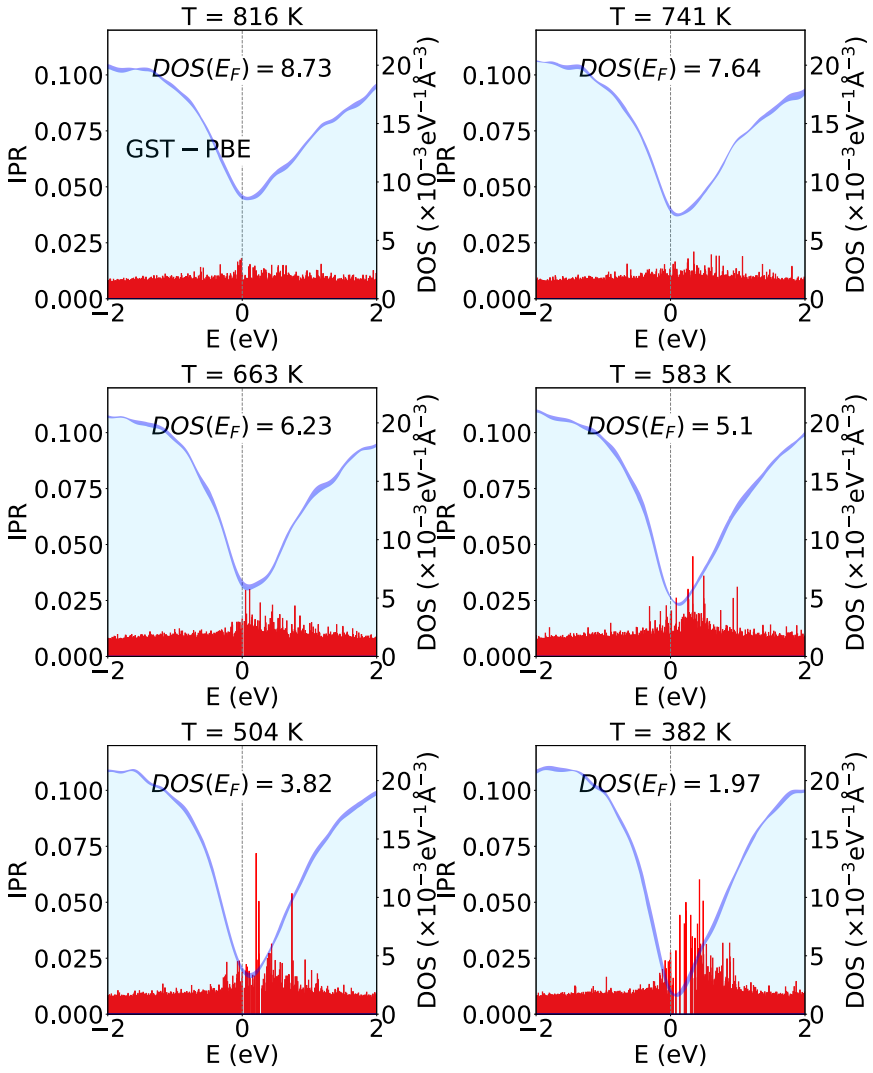


Fig. S4. Electronic density of states (DOS) around the Fermi level of the liquid and supercooled liquid GST models generated with the PBE functional at different temperatures as reported in Fig. S3 with the Inverse participation Ratio (IPR) superimposed to highlight the rising of localized states in the pseudogap as temperature is lowered. The IPR refers to the same nine configurations used to compute the DOS. The value of the DOS at the Fermi level is given in each panel.

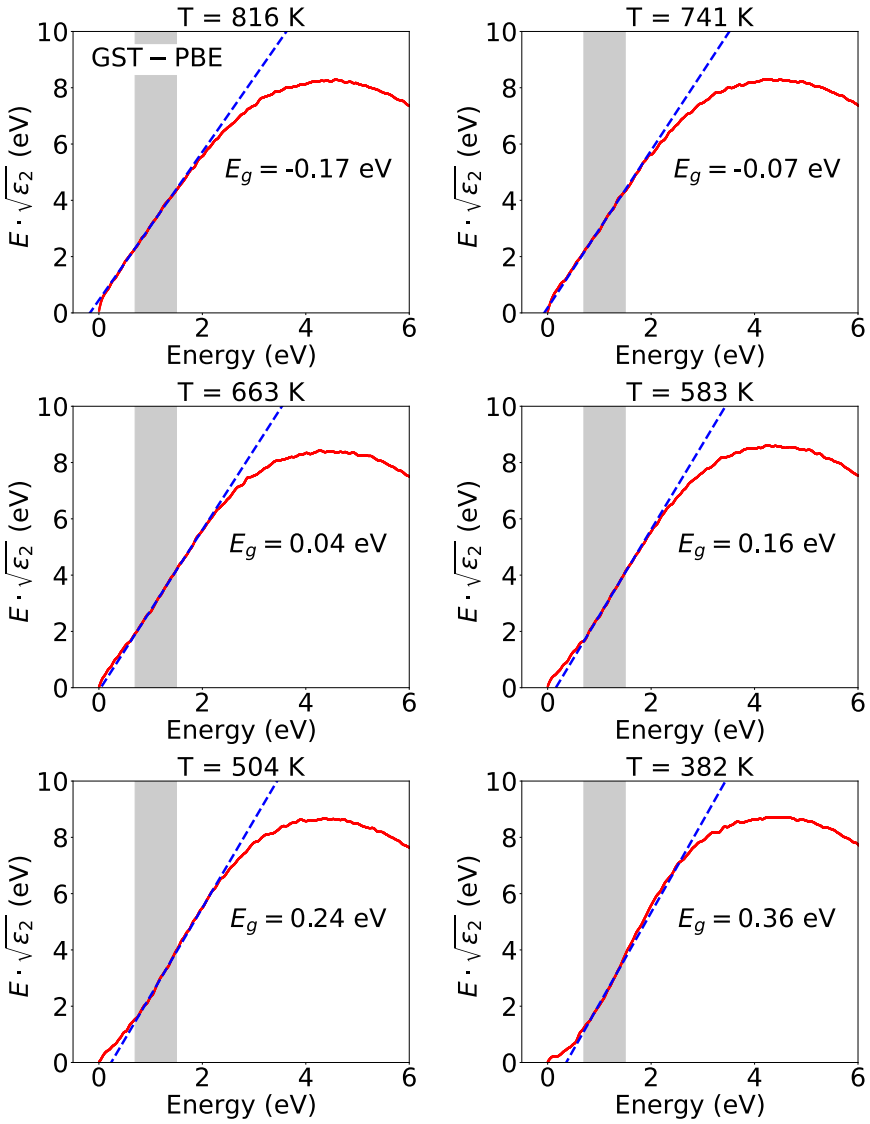


Fig. S5. Tauc plot of liquid and supercooled liquid GST at different temperatures obtained from PBE trajectories. The function $\varepsilon_2(E)$ is averaged over the same different configurations used for the DOS in Fig. S2. The dielectric function involves only energy differences and thus it does not depend on the choice of the alignment of the DOS in Fig. S2. The shaded area is used for the linear fitting. The resulting Tauc gap are given in each panel. The HSE06 functional was used to compute KS energies.

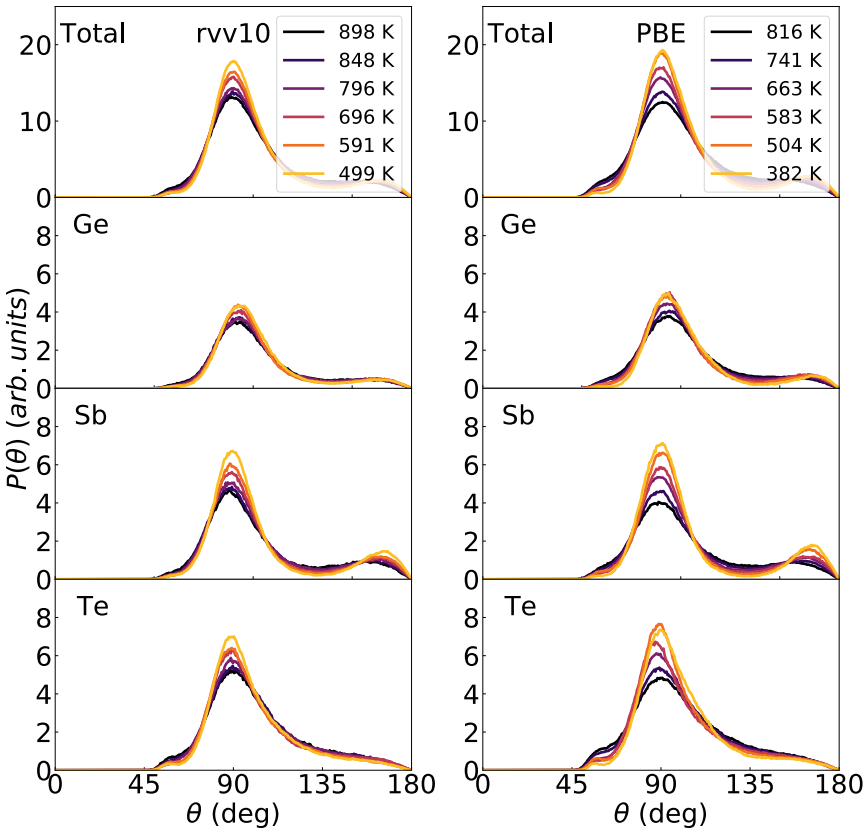


Fig. S6. Bond angle distribution function at different temperatures around different atomic species in liquid and supercooled liquid GST models generated with the (left) rVV10 and (right) PBE functionals. The cutoff for the definition of the bonds are 3.0, 3.0, 3.2, 3.2, 3.4, and 3.2 Å for Ge-Ge, Ge-Sb, Ge-Te, Sb-Sb, Sb-Te and Te-Te pairs.

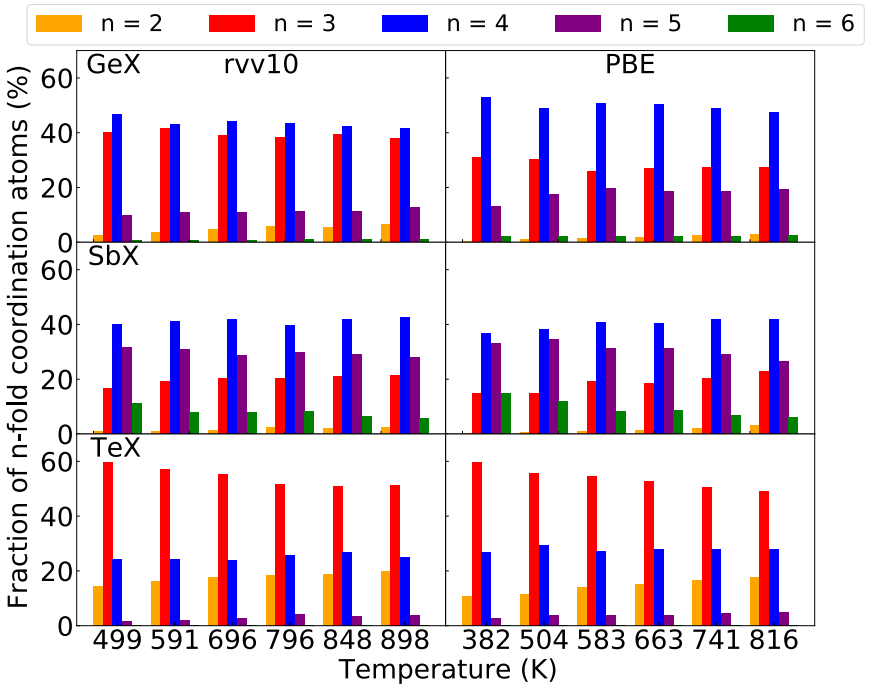


Fig. S7. Distribution of coordination numbers at different temperatures for atomic species in liquid and supercooled liquid GST models generated with the (a-b) rVV10 and (c-d) PBE functionals.

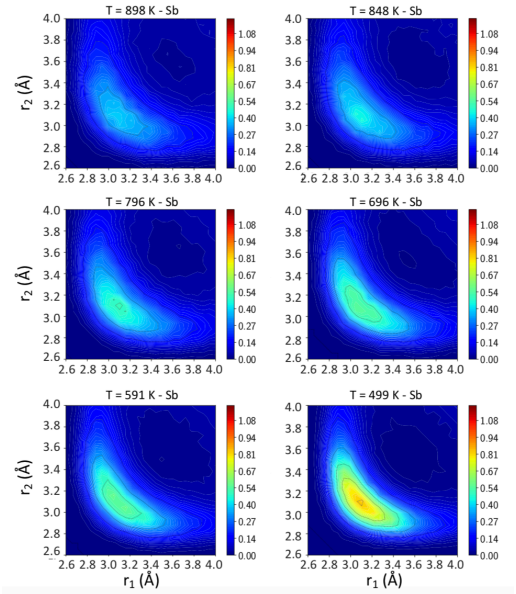


Fig. S8. ALTBC function for $Ge_2Sb_2Te_5$ for Sb atoms for the rVV10 simulations at different temperatures. Radial distances $r_1$ and $r_2$ are in Å.

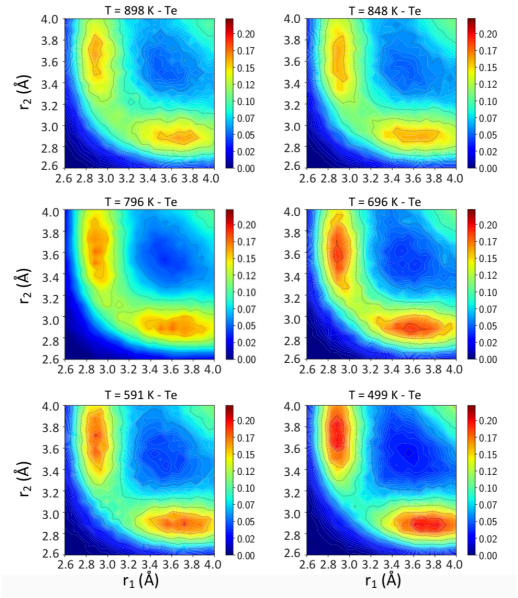


Fig. S9. ALTBC function for $Ge_2Sb_2Te_5$ for Te atoms for the rVV10 simulations at different temperatures. Radial distances $r_1$ and $r_2$ are in Å.

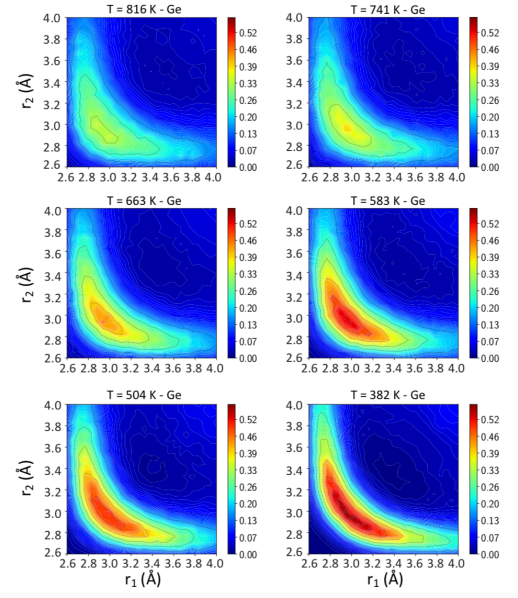


Fig. S10. ALTBC function for $Ge_2Sb_2Te_5$ for Ge atoms for the PBE simulations at different temperatures. Radial distances $r_1$ and $r_2$ are in Å.

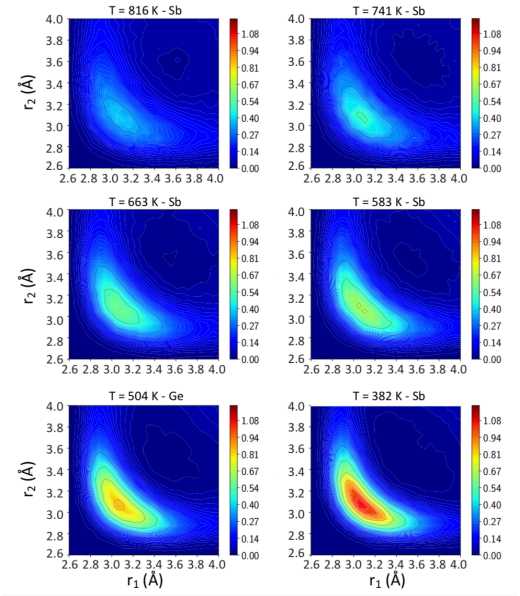


Fig. S 11. ALTBC function for $Ge_2Sb_2Te_5$ for Sb atoms for the PBE simulations at different temperatures. Radial distances $r_1$ and $r_2$ are in Å.

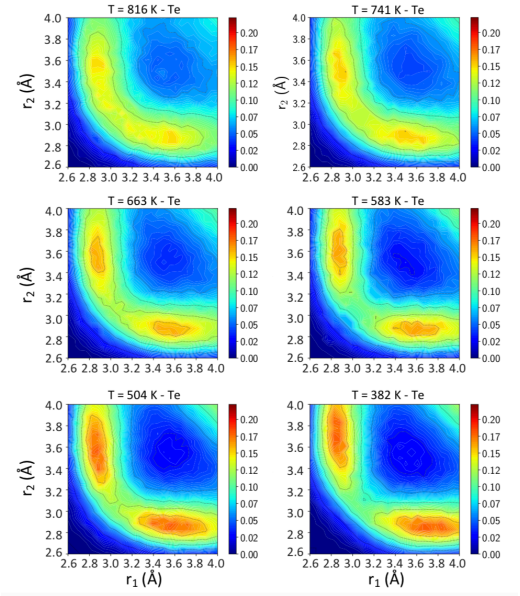


Fig. S 12. ALTBC function for $Ge_2Sb_2Te_5$ for Te atoms for the PBE simulations at different temperatures. Radial distances $r_1$ and $r_2$ are in Å.

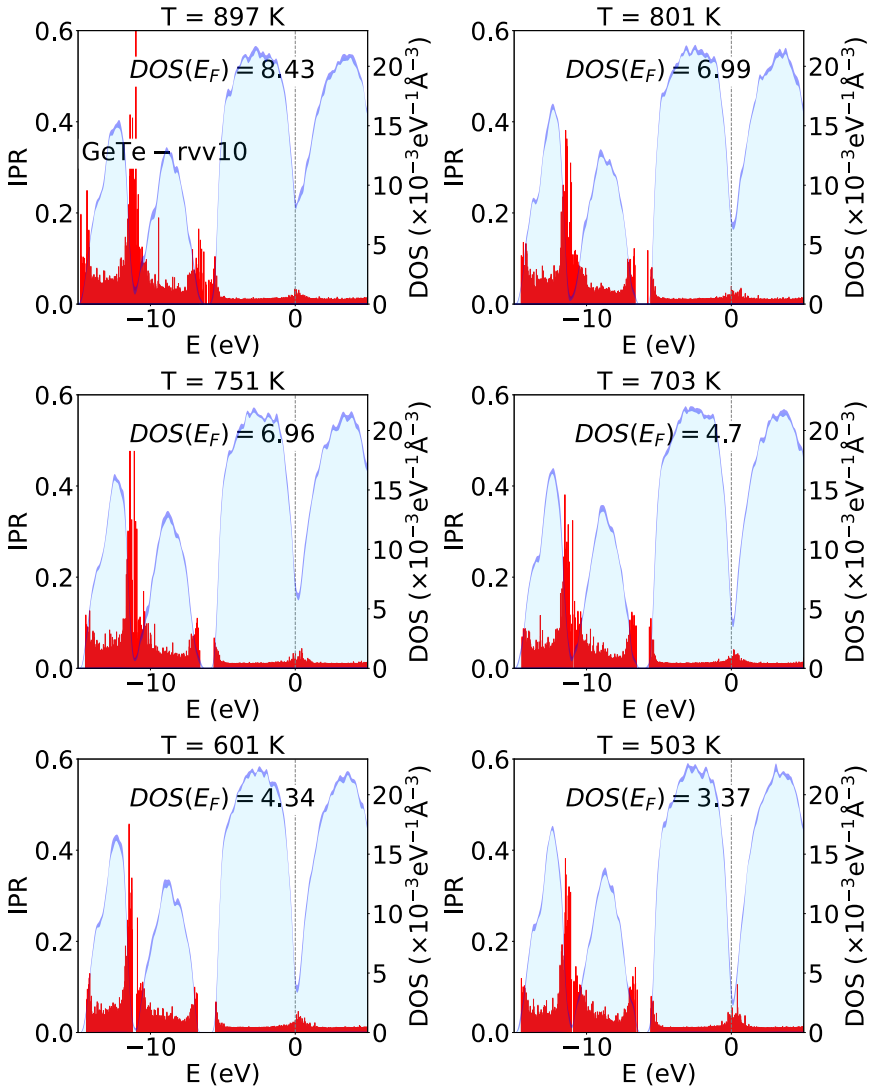


Fig. S13. Electronic density of states (DOS) around the Fermi level of the liquid and supercooled liquid GeTe models generated with the rVV10 functional at different temperatures. The DOS are obtained from Kohn-Sham energies computed with the HSE06 functional and broadened with Gaussian functions 27 meV wide. The DOS is averaged over nine configurations at each temperature, the DOS of the different configurations are aligned at the highest occupied state. Standard deviations are depicted by the blue shaded area around the solid lines. Different alignments of the DOS were also checked (see Section II in the article). The zero of energy is the Fermi level assigned by the average DOS at each temperature and the constraint on the total number of electrons. The Inverse participation Ratio (IPR) is superimposed. The IPR refers to the same nine configurations used to compute the DOS. The value of the DOS at the Fermi level is given in each panel.

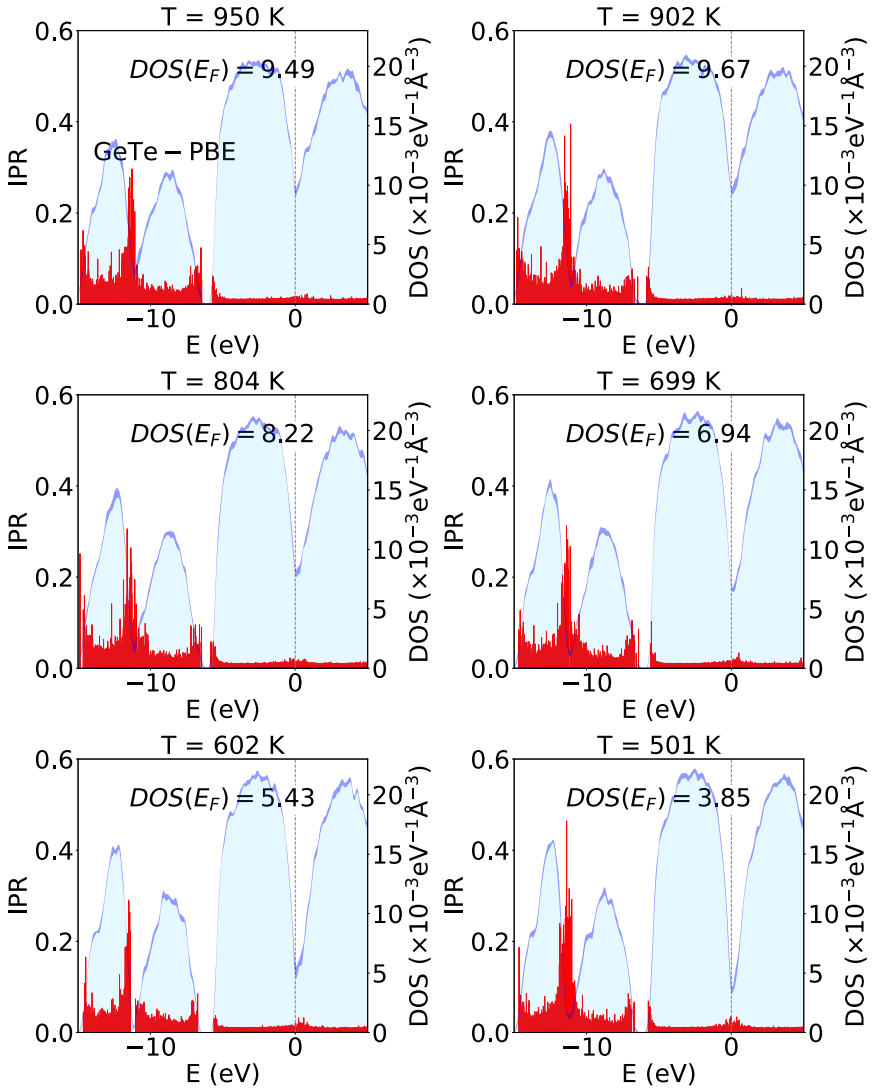


Fig. S14. Electronic density of states (DOS) around the Fermi level of the liquid and supercooled liquid GeTe models generated with the PBE functional at different temperatures. The DOS are obtained from Kohn-Sham energies computed with the HSE06 functional and broadened with Gaussian functions 27 meV wide. The DOS is averaged over nine configurations at each temperature, the DOS of the different configurations are aligned at the highest occupied state. Standard deviations are depicted by the blue shaded area around the solid lines. Different alignments of the DOS were also checked (see Section II in the article). The zero of energy is the Fermi level assigned by the average DOS at each temperature and the constraint on the total number of electrons. The Inverse participation Ratio (IPR) is superimposed. The IPR refer to the same nine configurations used to compute the DOS. The value of the DOS at the Fermi level is given in each panel.

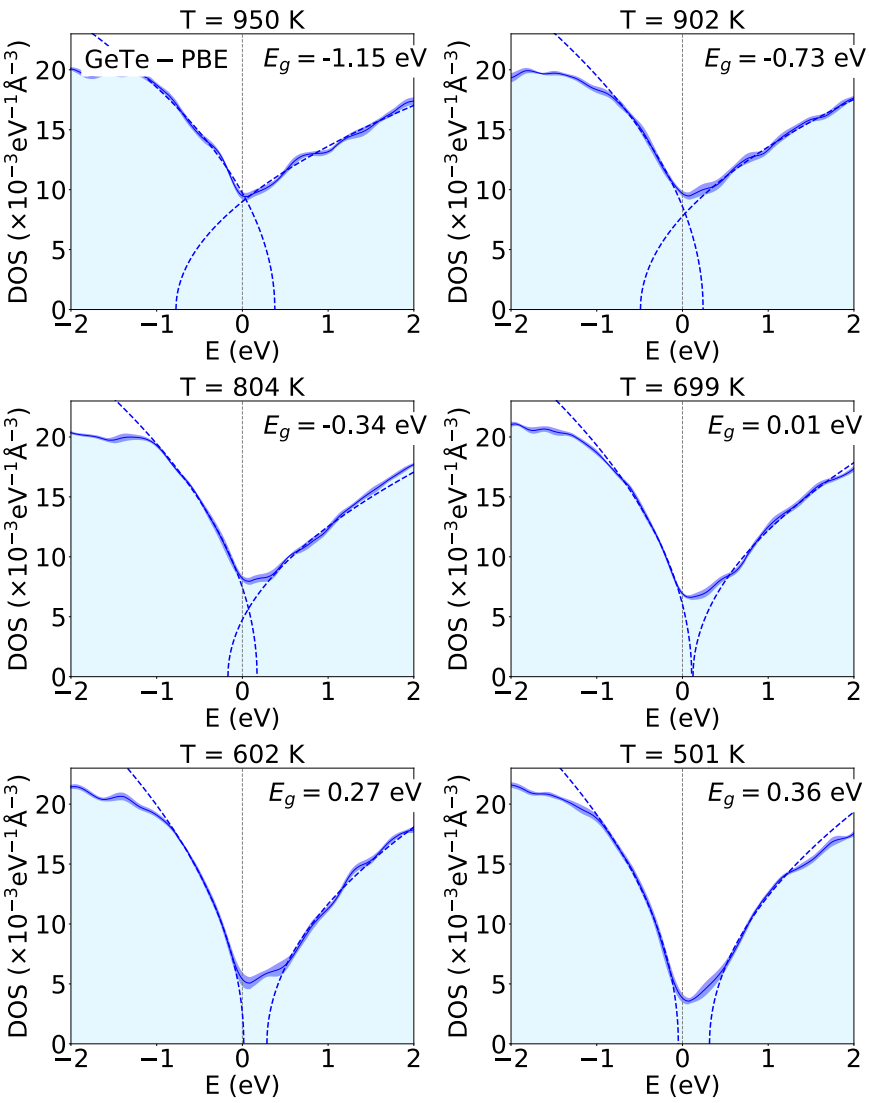


Fig. S15. Electronic density of states (DOS) around the Fermi level of the liquid and supercooled GeTe liquid models generated with the PBE functional at different temperatures (see Fig. S14). The DOS is averaged over nine configurations at each temperature, the DOS of the different configurations are aligned at the highest occupied state. Standard deviations are depicted by the blue shaded area around the solid lines. Different alignments of the DOS were also checked (see Section II in the article). The zero of energy is the Fermi level assigned by the average DOS at each temperature and the constraint on the total number of electrons. The fitting of the valence and conduction band edges with the square-root function $A_c\sqrt{E - E_c}$ and $A_v\sqrt{E_v - E}$ in the gray shaded regions are also shown (dashed lines). The fitting parameters $A_v$, $E_v$, $A_c$ and $E_c$ are given in Table SIV above. The resulting band gap $E_g$=$E_c$ -$E_v$ is given in each panel.

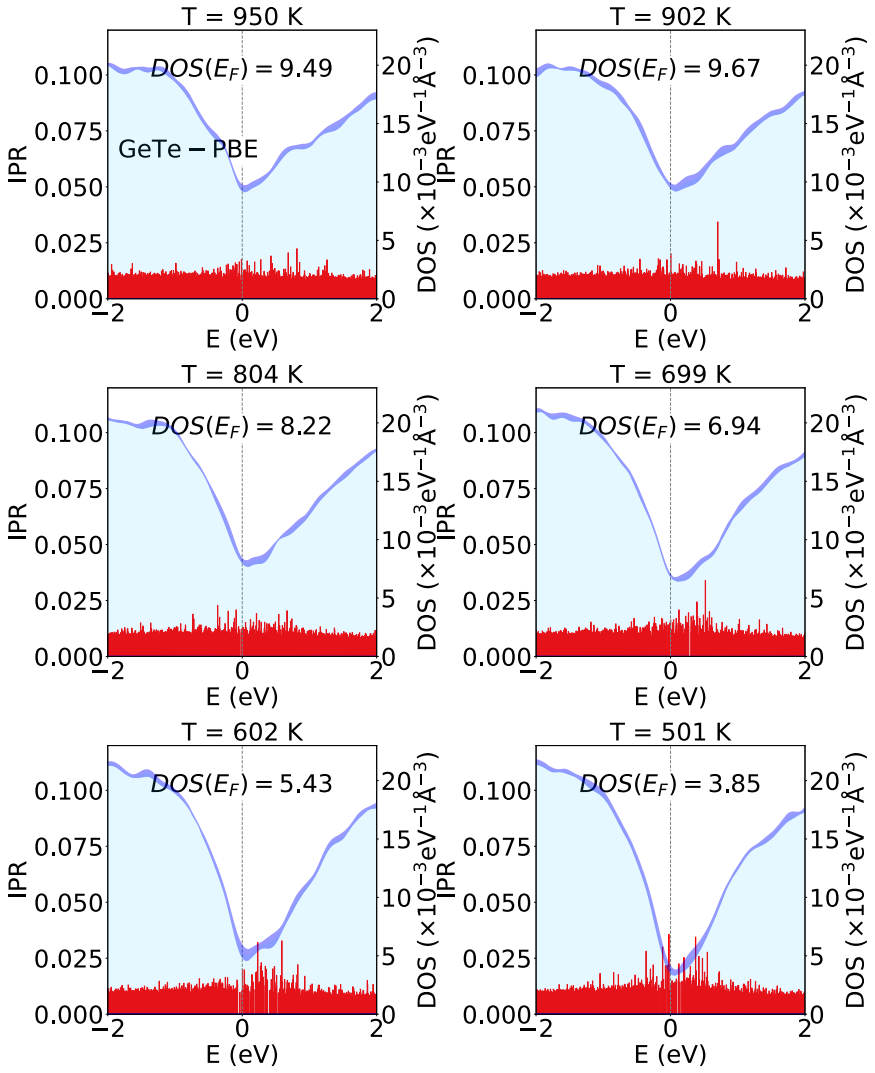


Fig. S16. Electronic density of states (DOS) around the Fermi level of the liquid and supercooled liquid GeTe models generated with the PBE functional at different temperatures as reported in Fig. S15 with the Inverse participation Ratio (IPR) superimposed to highlight the rising of localized states in the pseudogap as temperature is lowered. The IPR refers to the same nine configurations used to compute the DOS. The value of the DOS at the Fermi level is given in each panel.

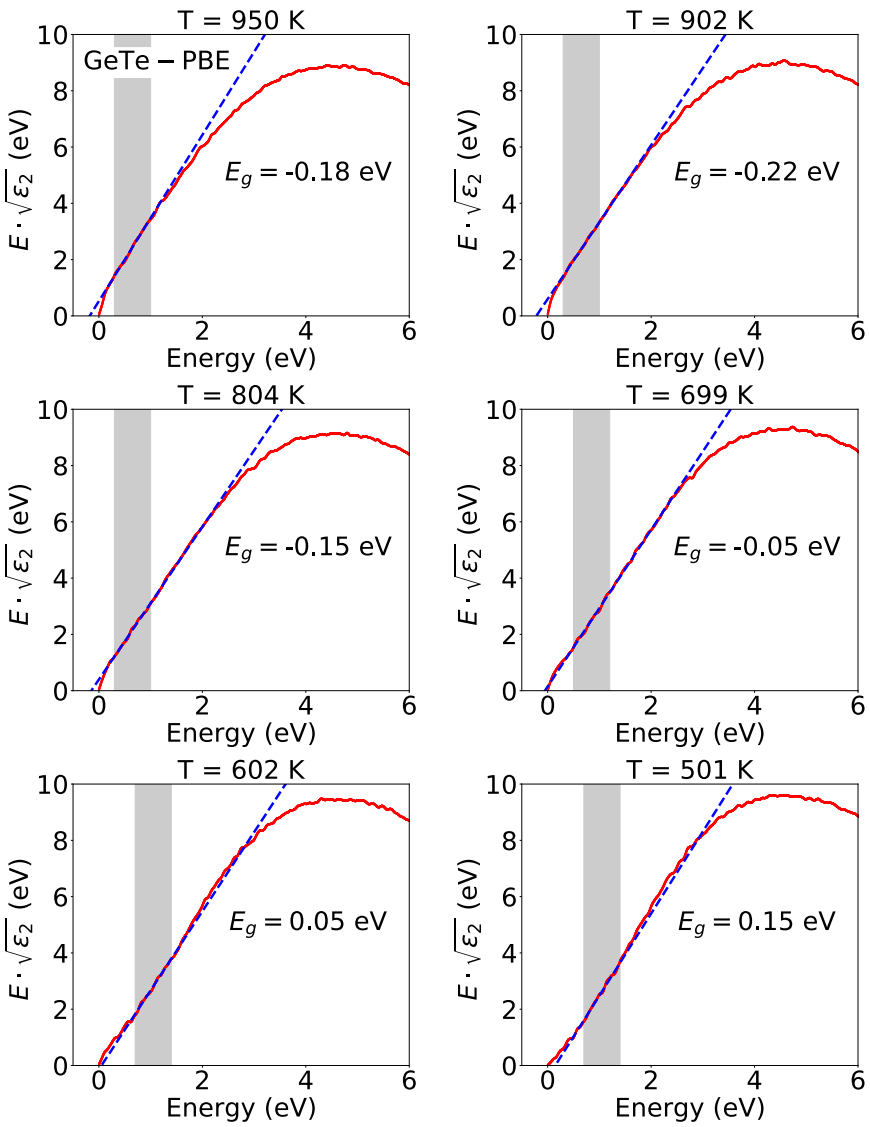


Fig. S17. Tauc plot of liquid and supercooled liquid GeTe at different temperatures obtained from PBE trajectories. The function $\varepsilon_2(E)$ is averaged over the same different configurations used for the DOS in Fig. S15. The dielectric function involves only energy differences and thus it does not depend on the choice of the alignment of the DOS in Fig. S15. The shaded area is used for the linear fitting. The resulting Tauc gap are given in each panel. The HSE06 functional was used to compute KS energies.

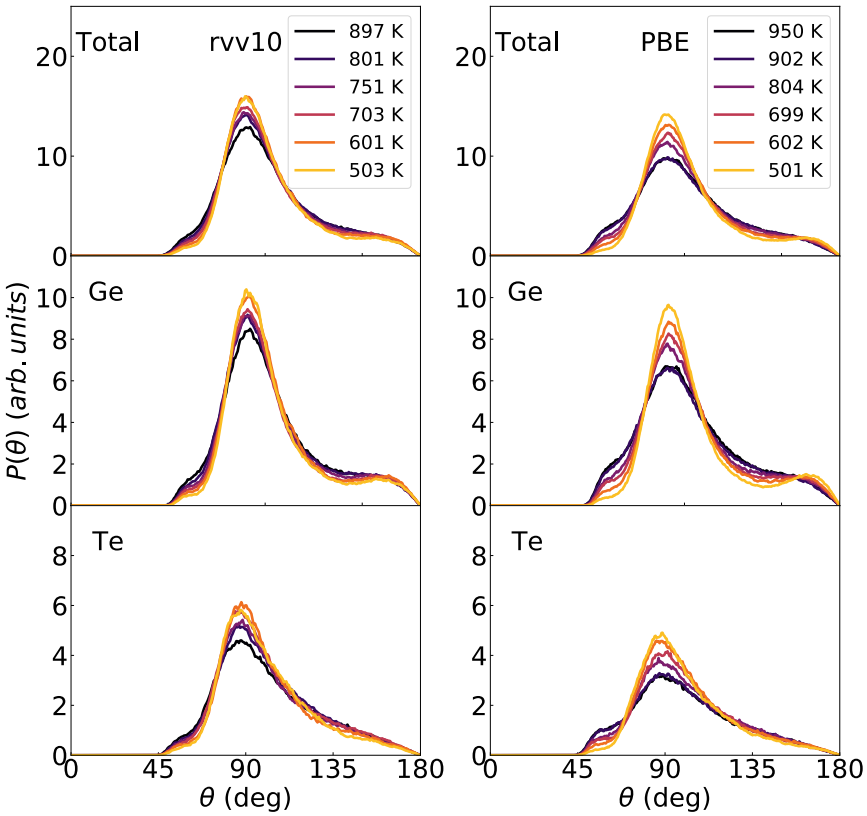


Fig. S18. Bond angle distribution function at different temperatures around different atomic species in liquid and supercooled liquid GeTe models generated with the (left) rVV10 and (right) PBE functionals. The cutoff for the definition of the bonds are 3.0, 3.22, and 3.0 Å for Ge-Ge, Ge-Te and Te-Te pairs.

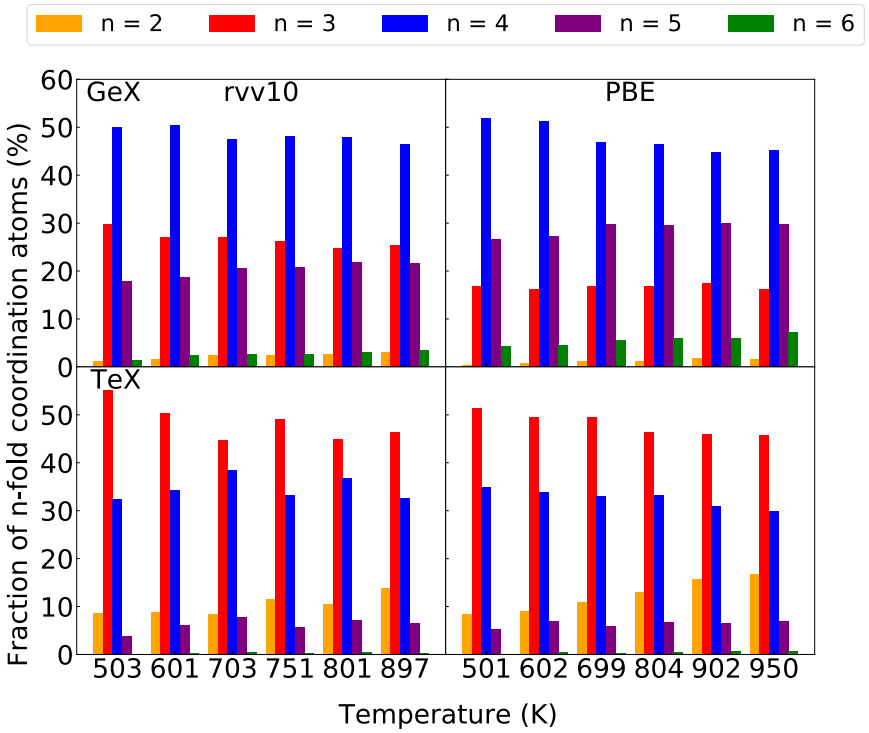


Fig. S19. Distribution of coordination numbers at different temperatures for atomic species in liquid and supercooled liquid GeTe models generated with the (a-b) rVV10 and (c-d) PBE functionals.

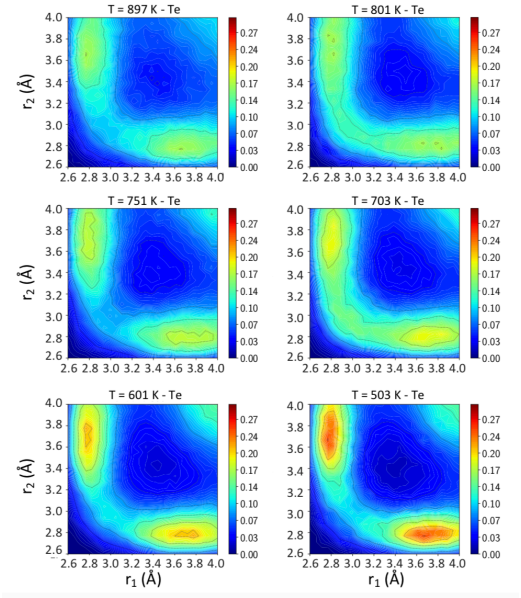


Fig. S20. ALTBC function for GeTe for Te atoms for the rVV10 simulations at different temperatures. Radial distances $r_1$ and $r_2$ are in Å.

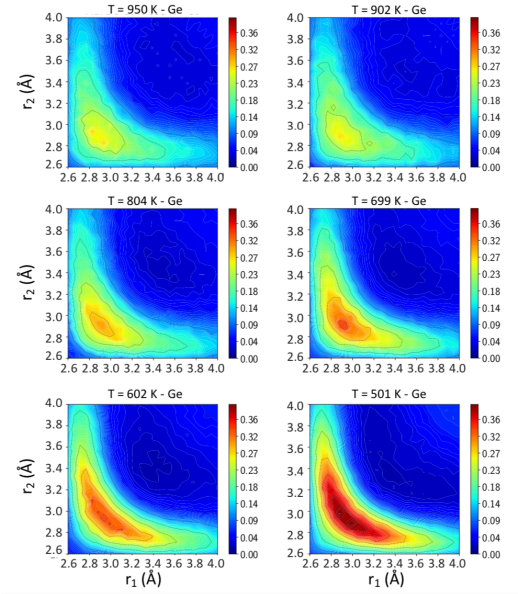


Fig. S21. ALTBC function for GeTe for Ge atoms for the PBE simulations at different temperatures. Radial distances $r_1$ and $r_2$ are in Å.

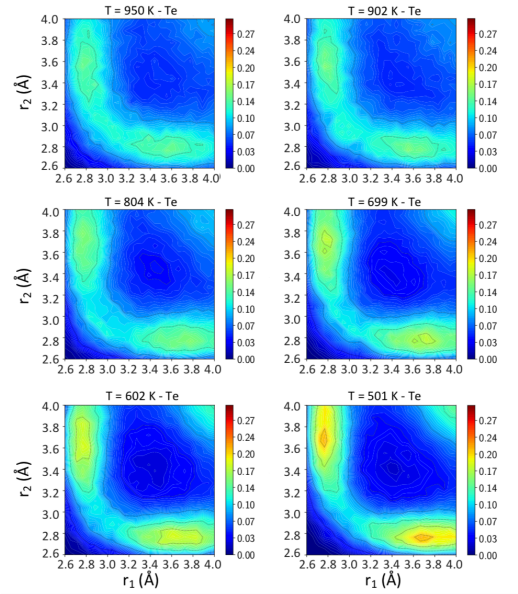


Fig. S22. ALTBC function for GeTe for Te atoms for the PBE simulations at different temperatures. Radial distances $r_1$ and $r_2$ are in Å.